Generalized Regression Neural Network Based Channel Identification and Compensation Using Scattered Pilot

He HE [1], Shun KOJIMA [1], Takaki OMURA [1], Kazuki MARUTA [2], Chang-Jun AHN [1]

[1] Graduate School of Engineering, Chiba University, Chiba 263-8522, Japan
[2] Academy for Super Smart Society, Tokyo Institute of Technology, Tokyo 152-8552, Japan

kakukaku@chiba-u.jp

Submitted September 15, 2020 / Accepted July 17, 2021

Abstract. *In the high-speed mobile environment, channel state information (CSI) estimated at the beginning of the packet is quite different at the last part because the actual channel state changes with time. To overcome this problem, a neural network (NN) based channel compensation method was previously developed. Due to inaccurate channel estimation of decision feedback channel estimation (DFCE), the pilot-aided CSI of the first symbol and DFCE-aided CSIs in the intermediate data part will cause inexact channel state transition even though the application of NN. Accordingly, the channel compensation performance is still degraded, especially in the last part of the packet. This paper proposes a new version of GRNN based channel identification and compensation method by introducing scattered pilot. It can improve the tracking capability of GRNN thanks to densely arranged pilot in the time-domain while it cannot reduce the transmission efficiency. Simulation results show that the proposed method is more effective than the conventional ones in terms of RMSE and BER performance, even in the fast fading environment.*

Keywords

OFDM, fast fading, channel estimation, generalized regression neural network, DFCE, scattered pilot

1. Introduction

With the rapid development of communication technology and the spread of a large number of mobile communication terminals, security and certainty of wireless communication services have attracted extensive attention. These are essential to achieve a reliable system for fifth generation (5G) mobile communication systems [1]. Packet based transmission based on orthogonal frequency division multiple (OFDM) is employed for a large majority of modern wireless communication systems such as long term evolution (LTE) and Wi-Fi. The quality of channel state information (CSI) directly impacts the performance of the entire system. Pilot-assisted channel estimation (PCE) [2] is one of the CE methods and is widely used. Meanwhile, this method cannot fully compensate for the fluctuation of channel state, i.e. amplitude and phase, caused by temporal fading. Under the fast fading environment, the channel state changes so rapidly that the CSI estimated by the PCE especially in the last part of the packet is largely different from the actual channel state. In order to trace the channel state transition, several approaches have been investigated. The periodic pilot-symbol-aided (PSA) channel estimation [3] is one of them. It requires a large complexity due to the detection methods. Earlier work in [4], [5] conceived the scattered pilot for the fast fading channel compensation. Scattered pilot has a great effect on fast fading channel. In the scattered pilot, the general one-dimensional interpolation method is usually performed in the frequency- or time-domains of the scattered pilot to reduce the amount of computation. However, it is difficult for the scattered pilot to interpolate in the deep faded channel, especially in the frequency domain. Moreover, if the coherence bandwidth is narrow relative to the interval of scattered pilot, the impulse responses will overlap when viewed in the time domain. To overcome these problems, a multilayer feedforward neural network (MLFNN) based channel estimation and compensation method was previously proposed in [6], [7]. This method employs MLFNN to compensate the channel variation through the generalization ability derived from the nonlinear relationship between input and output, and estimates the entire channel state transition. The MLFNN is trained using partially obtained CSI by the PCE and the data-aided decision feedback channel estimation (DFCE), where the PCE pilots are inserted at the head of the packet and the DFCE is applied to the middle part of the packet. The DFCE directly estimates channel variation at any specific data symbol using the difference between the received symbol and the replica symbol, which is the multiplication of remodulated symbol and CSI obtained by the PCE [8], [9]. However, it causes the processing delay due to the huge computation complexity imposed by the backpropagation (BP) training for the weight of the neural network [7]. The genetic algorithm [10], [11] and firefly algorithm (FFA) [12] can be applied to optimize the weight of the NN. Although these

approaches are reasonable to find an optimal solution, we need to repeat the iterative learning process which causes an unacceptable latency.

The improved version of this method was developed to replace MLFNN with a generalized regression neural network (GRNN) for NN part [13]. Due to its outperforming generalization capability, GRNN based channel estimation and compensation method can improve the transmission performance with less computation load. However, NNs still cannot estimate the accurate channel state transition due to the low reliability of desired responses. Especially as one of the desired responses, the estimated CSI by DFCE is sometimes incorrect due to decision errors when the channel state transition has a sharp fluctuation even in the beginning part of the packet.

In order to further improve the reliability of the desired responses without increasing the number of pilot symbols, we newly propose the modified version of GRNN based on the channel estimation method that the structure of pilot symbols is transformed and the CSI interpolated by DFCE in the frequency-domain is used as the desired responses for training. This method not only secures the resolution in the frequency domain, but also improves the tracking capability in the time-domain due to the scattered pilot. Since DFCE only refers to the front and back pilot signals in the time domain, even if one-dimensional interpolation is performed at the non-pilot position where data symbol is inserted, there is no need to consider the pilot spacing in the frequency domain and expands the scope of satisfying Nyquist sampling theorem by two times. It can also do better interpolation for deep fade than the general method [14], [15]. A key contribution of this paper is to increase reliability of the desired responses in NNs and to estimate the whole channel state transition accurately with maintaining the same transmission efficiency as well as computation complexity.

The rest of this paper is organized as follows. In Sec. 2, we overview the system model. Sections 3 and 4 describe the concept of DFCE and GRNN. Section 5 introduces the conventional GRNN based channel estimation scheme. Sections 6 and 7 present the proposed scheme and its performance through a computer simulation. Finally, Section 8 concludes this paper.

2. Channel Model

In this paper, we assume time varying multipath fading channel which is expressed as,

$$h(\tau, t) = \sum_{l=0}^{L-1} h_l(t)\delta(\tau - \tau_l) \tag{1}$$

where h_l denotes the complex channel coefficient and δ is the Dirac's delta function. L and τ_l indicate the number of discrete paths and the delay time, respectively. The normalized path gain is assumed here as $\sum_{l=0}^{L-1} \mathrm{E}|h_l^2| = 1$, where $\mathrm{E}|\cdot|$ indicates the ensemble average operation. The frequency response $H(f, t)$ via Fourier transform of the temporal impulse response can be obtained as,

$$H(f, t) = \int_{-\infty}^{\infty} h(\tau, t) \exp(-\mathrm{j}2\pi f\tau)\mathrm{d}\tau \tag{2}$$

$$= \sum_{l=0}^{L-1} h_l(t) \exp(-\mathrm{j}2\pi f\tau_l) \tag{3}$$

where f denotes the frequency. In a mobile communication environment, the frequency response is generally fluctuating. $L > 1$ provides frequency selective fading channel where $|H(f, t)|$ fluctuates in the transmission bandwidth [16], [17].

3. Decision Feedback Channel Estimation (DFCE)

DFCE is one of the channel estimation methods, and it uses the signals remodulated with DFCE and the reference CSI obtained by the pilot symbols inserted to the first symbol of the packet. The received signal of the k-th subcarrier and the i-th symbol, $Y(k, i)$, is represented and the white Gaussian noise $N(k, i)$ is added as follows:

$$\mathbf{Y}(k, i) = \mathbf{H}(k, i) \cdot \mathbf{X}(k, i) + \mathbf{N}(k, i). \tag{4}$$

First, the decision result of the transmitted symbol $\mathbf{D}'(k, i)$ is multiplied by the channel $\tilde{\mathbf{H}}(k)$ estimated from the pilot symbol to create a received signal replica $\mathbf{Y}_{\mathrm{rep}}(k, i)$. The channel variations $\Delta\mathbf{H}(k, i)$ is obtained by dividing the actual received signal $\mathbf{Y}(k, i)$ by the received signal replica $\mathbf{Y}_{\mathrm{rep}}(k, i)$. Furthermore, this channel variations $\Delta\mathbf{H}(k, i)$ is multiplied by the estimated channel $\tilde{\mathbf{H}}(k, i)$ to obtain the adjusted channel $\check{\mathbf{H}}(k, i)$. Finally, in order to reduce the noise which may result in a slight decrease of demodulation accuracy, the $(i - 1, i, i + 1)$th symbols of adjacent adjusted channel are also added and averaged together. Specifically, it is expressed by the following equations from (5) to (8).

$$\mathbf{Y}_{\mathrm{rep}}(k, i) = \tilde{\mathbf{H}}(k)\mathbf{D}'(k), \tag{5}$$

$$\Delta\mathbf{H}(k, i) = \frac{\mathbf{Y}(k, i)}{\mathbf{Y}_{\mathrm{rep}}(k, i)}, \tag{6}$$

$$\check{\mathbf{H}}(k, i) = \Delta\mathbf{H}(k, i) \cdot \tilde{\mathbf{H}}(k), \tag{7}$$

$$\hat{\mathbf{H}}(k, i) = \frac{\sum_{j=i-1}^{i+1} \check{\mathbf{H}}(k, j)}{3}. \tag{8}$$

However, decision errors are inevitable in this scheme resulting in inaccurate CSI estimation, especially under a fast fading environment where the channel variation from the front CSI given by PCE to the channel state in the last part of the packet is quite huge. Thus, applying DFCE to obtain the estimated CSI cannot improve compensation performance, especially in the last part of the packet.

4. Generalized Regression Neural Network (GRNN)

GRNN was proposed by Donald Specht in 1991, which evaluates the probability density function to solve the nonlinear approximation problem [18]. GRNN has excellent performances in both robust function approximation ability and learning speed. This is because it can provide convergence to the optimal regression surface rapidly by using a probability distribution, even though the sparse training samples included inaccurate responses [19]. Besides, GRNN directly sets weight value to training samples regarded as the expected value of response, instead of iterative learning to adjust the optimal value of the weight value [20–22].

As shown in Fig. 1, the GRNN is a parallel four-layer structure: input layer, pattern layer, summation layer, and output layer. The description of calculation flow is given as follows: the input neurons of input layer receives the input vector $\mathbf{x} = [x_1, x_2, \ldots, x_n]$. Then, the input neurons send these data to the pattern layer, which can realize the nonlinear transformation from the input space to the pattern space. The output of the i-th neuron in the pattern layer is expressed as

$$\phi_i(\mathbf{x}) = \exp\left(-\frac{\|\mathbf{x} - c_i\|^2}{2r^2}\right) \tag{9}$$

where r denotes the radius of the radial basis function (RBF) and c_i is a training input vector($1 \leq i \leq p$). p presents the number of training sets. r determines the generalization capability of the GRNN by controlling the degree of smoothness. When r is large, the ability to approximate dispersed training samples decreases due to smoother transitions. In contrast, when r becomes very small, the regression curve will change rapidly, causing a decrease in prediction ability.

The summation layer has two summations, called the simple summation S_s and the weighted summation S_w, respectively. S_s computes the arithmetic sum of the pattern layer outputs, expressed as

$$S_\mathrm{s} = \sum_{i=1}^{p} \phi_i(\mathbf{x}). \tag{10}$$

The k-th weighted summation S_w computes the weighted sum of the pattern layer outputs, expressed as

$$S_{\mathrm{w}k} = \sum_{i=1}^{p} y_i \phi_i(\mathbf{x}). \tag{11}$$

where y_i is interconnection weight in the i-th desired response.

After that, the output of the k-th output neuron in the GRNN model is calculated as follows by using (10) and (11) and represented as a weighted average of the desired responses.

$$\hat{y}_k = S_{\mathrm{w}k}/S_\mathrm{s}. \tag{12}$$

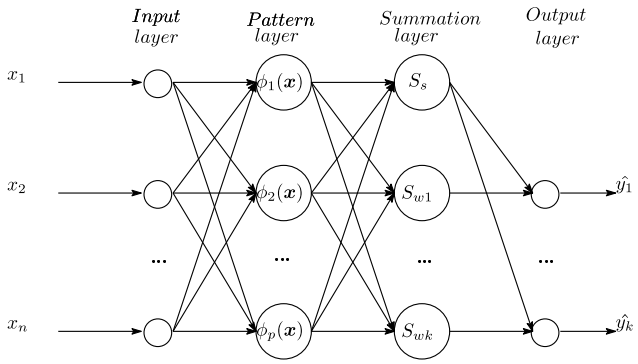

Fig. 1. Architecture of GRNN.

In addition, we compare the difference between MLFNN and GRNN. The MLFNN [7], [10–12] has to renew parameters iteratively in BP training until any training parameter reaches the target value. From this reason, the iterative process makes the computational complexity enormous and results in processing delay. In particular, the simulation results in paper [7] [13] have proved that the BP neural network needs to optimize several parameters by iteration to achieve the optimization of BER characteristics. In order to eliminate the iterative training process without imparing the generalization capability, we previously proposed the improving NN approach which employs GRNN for the NN part [13]. Different from the MLFNN back-propagation training that needs iterative weight update process, the desired response y_i of the training sets in the GRNN can be exploited for the weights directly like (11). Therefore its learning time can be reduced significantly.

To support this claim, we measured the calculation time from training to predict the channel state by MLFNN and GRNN in MATLAB. The channel estimation method is introduced in detail in the next section. Computation environment is Intel Core i5-CPU and 8GB RAM. The running time for GRNN is 5.912 ms, whereas that for MLFNN is 483.626 ms. As a result, GRNN can drastically reduce the calculation delay and it could fall within a feasible execution time with the hardware implementation. Our research focuses on execution time, and the conventional MLFNN cannot be applicable for the practical use due to its large amount of computation time. The main objective of this study is to provide a quantitative comparison between the pilot subcarrier interpolation methods based on GRNN aided channel state tracking.

5. Conventional GRNN Based Channel Estimation

Since the reliability of DFCE in the last part of the packet is low, the conventional GRNN based channel estimation is exploited to improve this problem [13]. This method only uses the CSIs partially obtained by the pilots inserted at the first symbol of the packet and that by DFCE in the intermediate data part of the packet, to employ the GRNN for

channel identification and compensation. The pilot pattern of the conventional method is shown in Fig. 2. Because of the nonlinear generalization capabilities, GRNN can be trained by only a few estimated CSIs to accurately trace the whole CSI transition. In addition, this approach unnecessitates to repeat the iterative learning process.

Figure 3 presents the block diagram of channel estimation based on GRNN when the number of symbols is N_t and the number of subcarriers is N_f. GRNN can predict an arbitrary function which has the relationship between the input vector and the desired responses by the training. Here, we set time-domain symbol indices $[1, 2, \ldots, N_t]$ as the input and frequency-domain channel responses $\mathbf{H}_{\text{out}}$ are set as the GRNN output. During the GRNN training as a regression function, indices $[1,\ s]$ are set as the training inputs where s denotes the arbitrary symbol index. The 1st desired response and the 2th one are set as CSIs estimated by PCE for the 1st symbol and by DFCE for the s-th symbol, respectively. In addition, the training inputs are the center of each RBF in the pattern layer. The desired responses are to be the weight of weighted summation directly in the summation layer. As a result, it does not need to learn to adjust the weights like MLFNN which must repeat the iterative learning process. Moreover, although the CSI contains real and imaginary parts, the desired responses can be directly set as the weight of complex value in (11), without being divided into two parts for the desired responses such as MLFNN.

In the prediction phase, the vector composing of indices for the whole symbols $[1, 2, \ldots, N_t]$ are input to GRNN. Each output of GRNN ($m = 1, 2, \ldots, N_f$) corresponds to the m-th subcarrier's CSI which is the complex value. Therefore, all of outputs of GRNN can present the whole channel state transition as follows,

$$\mathbf{H}_{\text{out}} = \begin{bmatrix} h_{\text{out}}(1,1) & \cdots & h_{\text{out}}(1,N_t) \\ \vdots & \ddots & \vdots \\ h_{\text{out}}(N_f,1) & \cdots & h_{\text{out}}(N_f,N_t) \end{bmatrix}. \quad (13)$$

However, under the fast fading environment, the channel state transition even in the beginning part is rapid so that the CSI estimated by only DFCE may also be inaccurate even if DFCE is conducted in the beginning part of the packet. Furthermore, GRNN trained by this inaccurate information as the desired responses cannot correctly compensate for the channel variation especially in the last part of the packet. Therefore, any method is needed for enhancing the reliability of desired responses and further improving the performance of channel compensation. Different from the conventional method that the CSIs in the s-th symbol are all estimated by DFCE, we introduce the following proposed method in the pilot pattern of Fig. 4.

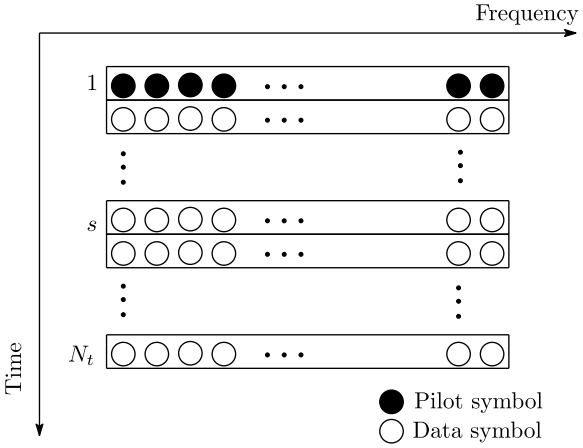

Fig. 2. Conventional pilot pattern.

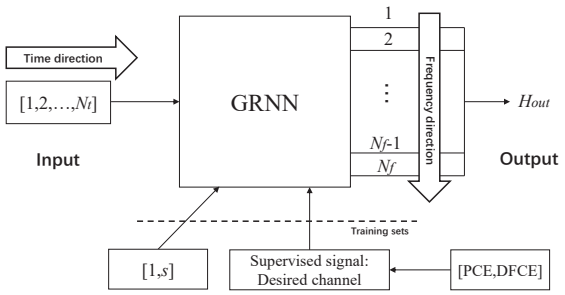

Fig. 3. Block diagram of channel estimation based on GRNN.

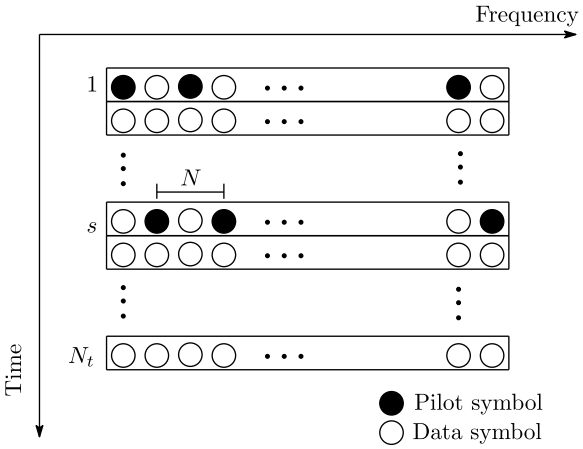

Fig. 4. Scattered pilot pattern.

6. Proposed System

In order to improve the reliability of the desired responses for the time variation, we incorporate the scattered pilot into the GRNN based channel identification and compensation. The conventional GRNN based channel estimation used only two spare training sets to estimate the whole transition of channel state because of the generalization ability of GRNN. Therefore, a modified scheme is proposed for the training set.

6.1 Scattered Pilot

In order to have an excellent ability to follow time fluctuations, the scattered pilot shown in Fig. 4 is employed. Different from the conventional method that the pilots are inserted at the head of the packet, the proposed scattered pilot is that the pilots are distributed in the front and first half of the packets. In other words, the pilots are inserted into every other subcarrier in the 1st and the s-th symbols. Since the same number of pilots as the conventional method is used, this scattered pilot pattern can maintain the signal transmission efficiency. In addition, since half of the pilots are shifted from the first symbol to the s-th symbol as the second desired response, it can not only ensure the resolution in the frequency domain, but also raise the stability of the desired response required for GRNN, which is superior to track the channel changes over time.

6.2 DFCE in the Scattered Pilot

DFCE implemented in the scattered pilot is different from the pilots set at the head of packet structure. At the 1st or the s-th symbols, the m-th null pilots ($m = 1, \ldots, N_f/2$) is interpolated by the DFCE which makes the decision from the channel $\tilde{\mathbf{H}}_{\mathrm{P}}(m)$ obtained by m-th pilot signals at the s-th symbol or 1st symbol, respectively. Equations (5) and (7) are changed as follows and the process is shown in Fig. 5.

$$\mathbf{Y}_{\mathrm{rep}}(k,i) = \tilde{\mathbf{H}}_{\mathrm{P}}(m,o)\mathbf{D}'(k,i), \tag{14}$$

$$\check{\mathbf{H}}(k,i) = \Delta\mathbf{H}(k,i) \cdot \tilde{\mathbf{H}}_{\mathrm{P}}(m,o) \tag{15}$$

where $o = 1$ or $o = s$, $k = 2m - 1$ or $k = 2m$.

6.3 The Improved Version of GRNN Based Channel Identification and Compensation Method

The proposed scheme then employs GRNN to compensate channel transition using the scattered pilot. In our proposal, the pilot symbol is inserted to the 1st and the s-th symbol as shown in Fig. 5. Thanks to the scattered pilot set in the beginning part of the packet, we can diminish the influence of decision error by leveraging CSI of the 2nd desired response corresponding to the s-th symbol. Due to the higher reliability of desired symbols, GRNN estimates whole channel state transitions more precisely than the previous scheme.

Figure 6 represents the procedure of the proposed scheme. These steps are similar to the conventional GRNN method until GRNN training. After interpolation process, the interpolated CSIs $\hat{\mathbf{H}}_{\mathrm{SP}}$ which are set as the desired responses are shown as

$$\hat{\mathbf{H}}_{\mathrm{SP}}(2m-1,1) = \tilde{\mathbf{H}}_{\mathrm{P}}(m,1), \tag{16}$$

$$\hat{\mathbf{H}}_{\mathrm{SP}}(2m,1) = \hat{\mathbf{H}}(2m,1), \tag{17}$$

$$\hat{\mathbf{H}}_{\mathrm{SP}}(2m,s) = \tilde{\mathbf{H}}_{\mathrm{P}}(m,s), \tag{18}$$

$$\hat{\mathbf{H}}_{\mathrm{SP}}(2m-1,s) = \hat{\mathbf{H}}(2m-1,s). \tag{19}$$

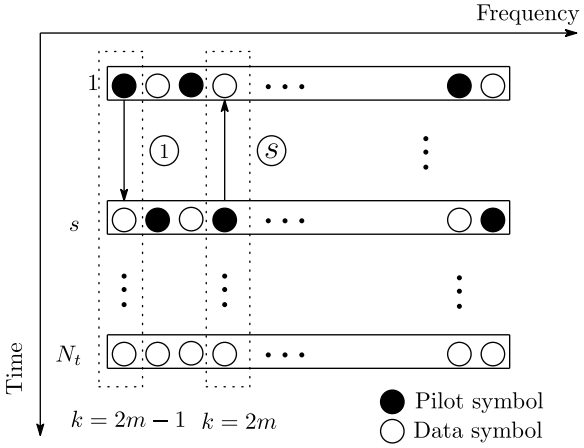

Fig. 5. DFCE in the scattered pilot.

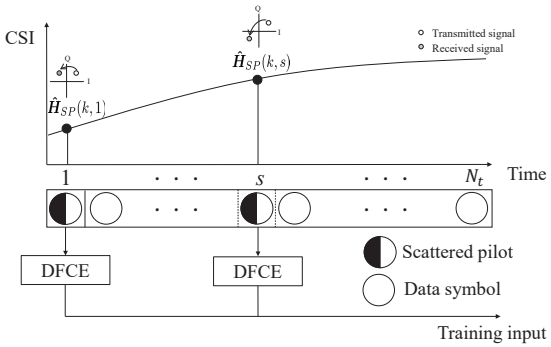

Fig. 6. The flow of channel estimation based on GRNN.

Then, $[1, s]$ are defined as the training inputs. Lastly, just like the conventional scheme, the vector composed of indices for all data symbols are input to the GRNN. Thanks to improving the reliability of the desired responses, GRNN outputs $\mathbf{H}_{\mathrm{out}}$ more accurately and we can use this information for channel compensation.

6.4 Comparison of DFCE and General Interpolation Method in the Scattered Pilot

Prior to employing GRNN to train, the general one-dimensional interpolation in the frequency-domain could also be used such as linear, spline and other interpolation approaches [23]. The interpolated CSI is regarded as the desired response of GRNN. If the CSI of the pilot signals in the frequency domain is directly used for interpolation, the Nyquist sampling theorem must be met as follows [24–26],

$$\tau_{\max} \cdot \triangle F \cdot N_i \leq 1 \tag{20}$$

where $\tau_{\max}$ is the maximum multipath delay time, $\triangle F$ is subcarrier spacing, N_i is the interval of adjacent pilot in the frequency-domain. For example, the Nyquist law is to keep the impulse responses in the time domain without overlapping as shown in Fig. 7(a). On the other hand, the excessive pilot interval causes overlap of impulse responses, i.e. aliasing, as shown in Fig. 7(b) and it complicates interpolating CSI for nullified subcarriers.

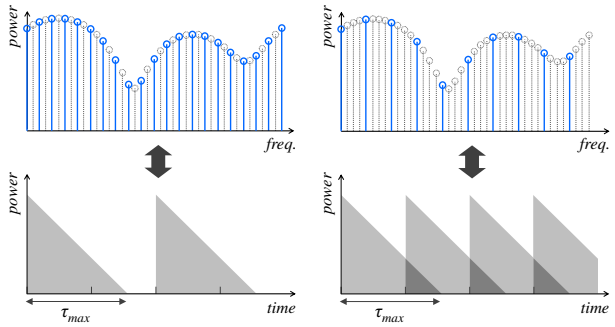

(a) $N_i = 2$ (b) $N_i = 4$

Fig. 7. Time and frequency representations of channel.

For DFCE interpolation in the frequency domain, as long as each subcarrier has a pilot in the frequency domain, the range of Nyquist law is the same as the conventional method of placing the pilot at the beginning of the packet expressed as follows,

$$\tau_{\max} \cdot \triangle F \leq 1. \tag{21}$$

This is because DFCE refers to the pilot information in the front and back time directions and no matter what the interval N_i is. Accordingly, the CSI of the whole subcarriers can be calculated by DFCE. For example, the pilots are distributed as shown in Fig. 4. When the subcarriers of the frequency domain without any pilots in the s-th symbol are interpolated by the general one-dimensional interpolation method like spline interpolation, the Nyquist theorem must be met as follows and the spacing of the pilots in the frequency-domain must be considered as follows,

$$\tau_{\max} \cdot \triangle F \leq \frac{1}{2} \tag{22}$$

where the interval in the frequency domain is $N_i = 2$. This is because only the CSI of the pilot signal of the s-th symbol is used for interpolation in the frequency domain. But for DFCE, when the CSI of the pilot signal corresponding to the first symbol is used to implement DFCE, the place where there is no pilot in the s-th symbol is interpolated by the DFCE as formulated in (14), (15) and (19). Accordingly, the range of satisfying the Nyquist theorem is doubled like (21). In other words, since the CSI of the pilots in the time-domain is used to interpolate instead of using the CSI of the adjacent pilot in the frequency-domain, only the subcarrier spacing $\triangle F$ is considered, and there is no need to consider the interval of pilots N_i in the frequency domain.

7. Computer Simulation

7.1 Simulation Parameters

Table 1 summarizes the simulation parameters. The simulations are performed using MATLAB R2018a, an Intel Core i5 CPU at 3.00 GHz and 8 GB of memory storage. Transmission scheme is OFDM with 64 FFT points.

Parameters	Values
Transmission scheme	OFDM
Data modulation	QPSK
FFT size, Number of carriers	$N_f = 64$
Guard interval	16
Number of pilot symbols	$N_p = 1$
Number of data symbols	$N_t = 20$
Channel model	15 path Rayleigh fading, 1 dB decay
Max Doppler frequency	800 Hz
Transmission bandwidth	20 MHz
Forward error correction	Convolutional code ($R = 1/2$, $K = 7$)
Function of pattern layer	Gaussian

Tab. 1. Simulation Parameters.

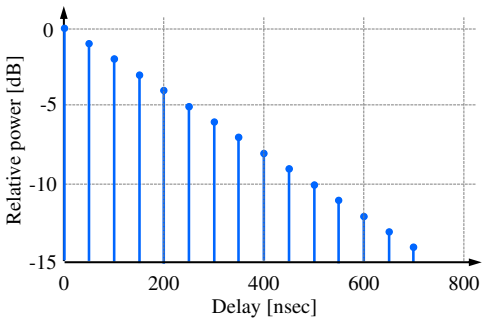

Fig. 8. Channel model.

The data stream is encoded by convolution codes ($R = 1/2, K = 7$). N_p and N_t denote the number of pilot and data symbols, respectively. The transmission bandwidth assumes 20 MHz and the OFDM symbol duration is 4 µs, including guard interval (GI), referred to the basic Wi-Fi specifications. The Jakes' fading model is used to represent time-varying channel. Suppose 15 multipaths, the average path gain of each is attenuated by 1 dB as shown in Fig. 8. Here, multipath time-delay is 50 ns. The maximum Doppler frequency is 800 Hz, which can indicate a fast fading environment. The scattered pilot structure assumed in the simulation is shown in Fig. 5. The pilots are set in the odd subcarriers of the first symbol and the even subcarriers of the s-th symbol, respectively.

7.2 Simulation Results

As the preliminary evaluation, we compare the scattered pilot method of DFCE with the general interpolation method which performs low-complexity interpolation in the frequency-domain. Here we use calculation time to compare the computation complexity as summarized in Tab. 2. The spline interpolation requires complex computation with all reference values and thus it takes twice as much time to interpolate CSI in the frequency-domain than DFCE. Therefore, DFCE-aided interpolation is computationally efficient.

Method	Calculation time
Spline	0.905 ms
DFCE	0.406 ms

Tab. 2. Computation time comparison

Root mean square error (RMSE) is then used to compare the interpolation accuracy with the CSI at the first symbol of the packet. In Fig. 9, the lowest RMSE values are presented when the DFCE method is applied to interpolate the CSI in the frequency domain. From this result, the DFCE method has the best performance and can be introduced into the desired response of GRNN in the proposed method.

Hereafter the optimum parameters for the conventional and the proposed methods are examined for fair comparison. Figure 10 presents the bit error rate (BER) versus radius of RBF r for the conventional method and the proposed method at $E_b/N_0 = 25$ dB and $s = 10$. When the radii of RBF r are 4.5 and 5, the conventional and the proposed methods show the best BER performance, respectively. The above parameters are used to verify the best parameters. Figure 11 presents the BER performance comparison with the position of the second scattered pilot at $E_b/N_0 = 25$ dB. Both methods achieve the best BER performance at $s = 10$. From this result, we apply parameters as $s = 10$ and $r = 4.5$ for the conventional method, and $s = 10$ and $r = 5$ for the proposed method.

Figure 12 shows the BER performances of the DFCE only, the conventional GRNN method and the proposed method. The BER performance of the DFCE significantly deteriorates because decision errors frequently happen in the last part of the packet. Although the conventional GRNN method can obtain more improved BER performance than that of the DFCE only, the error floor appears at around BER = 10^{-4}. The proposed approach removes the error floor and achieves the best BER performance below 10^{-5}. Based on this result, it was confirmed that the proposed method could improve the reliability of the desired response derived from the DFCE-aided interpolation of scattered pilot symbols. Therefore, channel tracking performance with compensation is greatly improved for all data symbols by GRNN, and

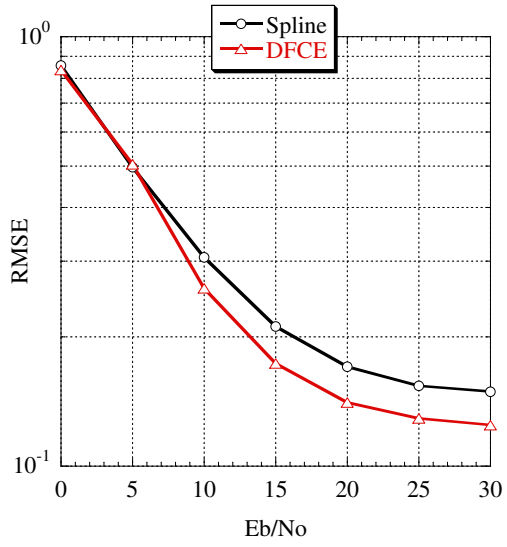

Fig. 9. RMSE vs. E_b/N_0 for the interpolation methods.

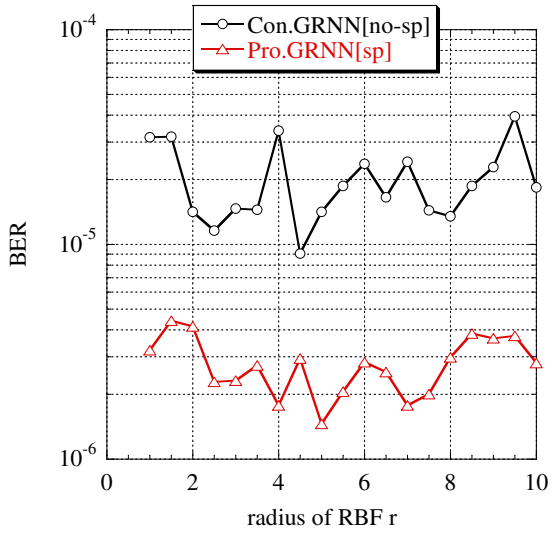

Fig. 10. BER vs. Radius of RBF r ($E_b/N_0 = 25$ dB, $s = 10$).

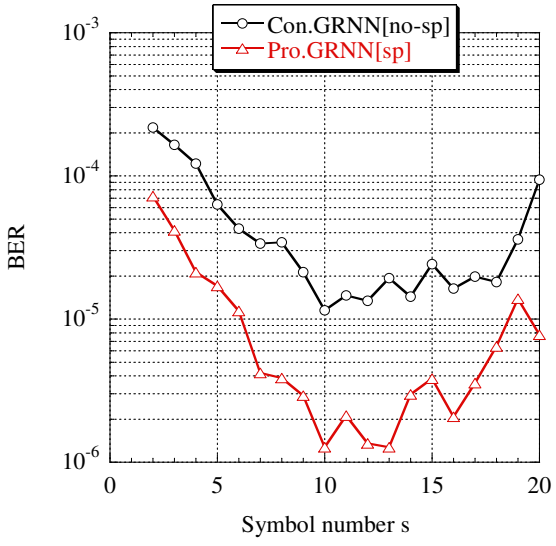

Fig. 11. BER vs. Symbol index s ($E_b/N_0 = 25$ dB).

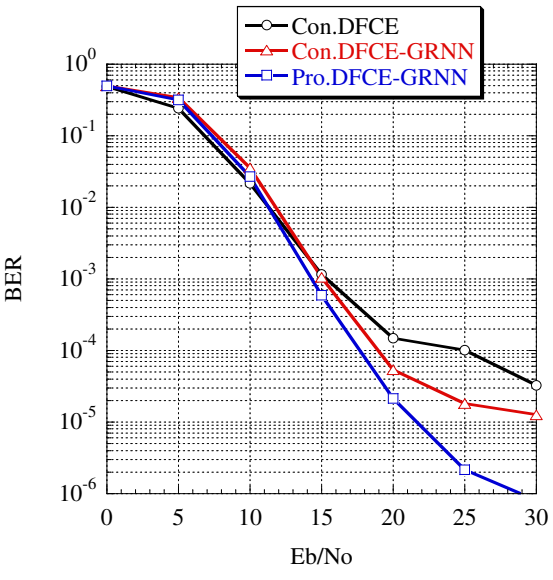

Fig. 12. BER vs. E_b/N_0.

the proposed system provides the superior channel tracking capability. From the above, it is shown that the DFCE method in the scattered pilot is quite effective under high mobility environment and has better performance than the conventional GRNN method and the general interpolation method.

8. Conclusion

In this paper, we proposed the GRNN based channel identification and compensation method using the scattered pilot to improve the reliability of the desired response for the GRNN. From the simulation results of the general low-complexity interpolation method and the proposed method comparisons, the proposed method is the most effective for interpolating in the frequency domain of the scattered pilot with lower computation complexity. Moreover, comparing the proposed method with the conventional method, the proposed method that changes the distribution of pilots can refine the performance of the desired response without degrading the transmission efficiency, thus improving the whole channel tracking performance of the GRNN. Through the computer simulation, the proposed method has shown the best BER performance compared with the DFCE only and the conventional GRNN method even at 800 Hz maximum Doppler frequency. Accordingly, we can conclude that the proposed method greatly enhances the effect of channel compensation, even in the high mobility environment.

References

[1] MARTIKAINEN, H., VIERING, I., et al. Mobility and reliability in LTE-5G dual connectivity scenarios. In *IEEE Vehicular Technology Conference (VTC-Fall)*. Toronto (Canada), 2017, p. 1–7. DOI: 10.1109/vtcfall.2017.8288056

[2] ALWAKEEL, A. S., MEHANA, A. H. Data-aided channel estimation for multiple-antenna users in massive MIMO systems. *IEEE Transactions on Vehicular Technology*, 2019, vol. 68, no. 11, p. 10752–10760. DOI: 10.1109/tvt.2019.2938344

[3] FUNADA, R., HARADA, H., KAMIO, Y., et al. A channel estimation method for a highly mobile OFDM wireless access system. *IEICE Transactions on Communications*, 2005, vol. E88-B, no. 1, p. 282–291. DOI: 10.1093/ietcom/e88-b.1.282

[4] HAYASHI, H., OKAMOTO, E., IWANAMI, Y. A fast fading channel estimation scheme for OFDM with sparse and scattered pilot symbols. In *International Symposium on Intelligent Signal Processing and Communication Systems (ISPACS)*. Kanazawa (Japan), 2009, p. 154–157. DOI: 10.1109/ISPACS.2009.5383877

[5] OUYANG, R., MATSUMURA, T., MIZUTANI, K., et al. A reliable channel estimation scheme using scattered pilot pattern for IEEE 802.22-based mobile communication system. *IEEE Transactions on Cognitive Communications and Networking*, 2019, vol. 5, no. 4, p. 935–948. DOI: 10.1109/tccn.2019.2930594

[6] OMURA, T., KOJIMA S., MARUTA, K., et al. Neural network based channel identification and compensation. In *International Symposium on Communications and Information Technologies (ISCIT)*. Bangkok (Thailand), 2018, p. 349–354. DOI: 10.1109/iscit.2018.8587981

[7] OMURA, T., KOJIMA S., MARUTA, K., et al. Neural network based channel identification and compensation. *IEICE Communications Express*, 2019, vol. 8, no. 10, p. 416–421. DOI: 10.1587/comex.2019XBL0095

[8] SOEJIMA, S., IDA, Y., AHN, C. J., et al. Fast fading compensation based on weighted channel variance for TFI-OFDM. *Journal of Signal Processing*, 2013, vol. 17, no. 3, p. 41–49. DOI: 10.2299/jsp.17.41

[9] YOFUNE, M., AHN, C. J., KAMIO, T., et al. Decision direct and linear prediction based fast fading compensation for TFIOFDM. *Far East Journal of Electronics and Communications*, 2009, vol. 3, no. 1, p. 35–52.

[10] CHENG, C. H., HUANG, Y. H., CHEN, H. C. Channel estimation in OFDM systems using neural network technology combined with a genetic algorithm. *Soft Computing*, 2016, vol. 20, no. 10, p. 4139–4148. DOI: 10.1007/s00500-015-1749-7

[11] SARWAR, A., SHAH, S. M., ZAFAR, I. Channel estimation in space time block coded MIMO-OFDM system using genetically evolved artificial neural network. In *International Bhurban Conference on Applied Sciences and Technology (IBCAST)*. Islamabad (Pakistan), 2020, p. 703–709. DOI: 10.1109/IBCAST47879.2020.9044539

[12] SAHU, P., MOHAPATRA, P., PANIGRAHI, S., et al. Neural network training using FFA and its variants for channel equalization. *International Journal of Computer Information Systems and Industrial Management Applications*, 2017, vol. 9, p. 257–264. ISSN: 2150-7988

[13] OMURA, T., HOEUR, N., MARUTA, K., et al. Improving ANN based channel identification and compensation using GRNN method under fast fading environment. In *International Conference on Advanced Technologies for Communications (ATC)*. Hanoi (Vietnam), 2019, p. 28–32. DOI: 10.1109/atc.2019.8924557

[14] COLERI, S., ERGEN, M., PURI, A., et al. Channel estimation techniques based on pilot arrangement in OFDM systems. *IEEE Transactions on Broadcasting*, 2002, vol. 48, no. 3, p. 223–229. DOI: 10.1109/tbc.2002.804034

[15] STERBA, J., KOCUR, D. Pilot symbol aided channel estimation for ofdm system in frequency selective Rayleigh fading channel. In *International Conference Radioelektronika*. Bratislava (Slovakia), 2009, p. 77–80. DOI: 10.1109/radioelek.2009.5158729

[16] GOLDSMITH, A. *Wireless Communications*. Cambridge University Press, 2005. ISBN: 9787115170491

[17] GHASSEMLOOY, Z., POPOOLA, W., RAJBHANDARI, S. *Optical Wireless Communications: System and Channel Modelling with MATLAB*. CRC Press, 2017. ISBN: 9781138074804

[18] SPECHT, D. F. General regression neural network. *IEEE Transactions on Neural Networks*, 1991, vol. 2, no. 6, p. 568–576. DOI: 10.1142/9789812796851-0008

[19] AMIRI, M., DAVANDE, H., SADEGHIAN, A. et al Feedback associative memory based on a new hybrid model of generalized regression and self-feedback neural networks. *Neural Networks*, 2010, vol. 23, no. 7, p. 892–904. DOI: 10.1016/j.neunet.2010.05.005

[20] QI, J., JIANG, G., LI, G., et al. Surface EMG hand gesture recognition system based on PCA and GRNN. *Neural Computing and Applications*, 2020, vol. 32, no. 10, p. 6343–6351. DOI: 10.1007/s00521-019-04142-8

[21] GHRITLAHRE, H. K., PRASAD, R. K. Exergetic performance prediction of solar air heater using MLP, GRNN and RBF models of artificial neural network technique. *Journal of Environmental Management*, 2018, vol. 223, p. 566–575. DOI: 10.1016/j.jenvman.2018.06.033

[22] NETO, M. C. A., ARAUJO, J. P. L., MOTA, R. J. S., et al. Design and synthesis of an ultra wide band FSS for mm-wave application via general regression neural network and multiobjective bat algorithm. *Journal of Microwaves, Optoelectronics and Electromagnetic Applications*, 2019, vol. 18, no. 4, p. 530–544. DOI: 10.1590/2179-10742019v18i41729

[23] MAKKAR, R., SONI, S., BACHKANIWALA, A. K., et al. Pilot interpolation based channel estimation for LTE systems. *Procedia Computer Science*, 2020, vol. 171, p. 2261–2266. DOI: 10.1016/j.procs.2020.04.244

[24] OZDEMIR, M. K., ARSLAN, H. Channel estimation for wireless OFDM systems. *IEEE Communications Surveys and Tutorials*, 2007, vol. 9, no. 2, p. 18–48. DOI: 10.1109/comst.2007.382406

[25] ZERHOUNI, K., ELBAHHAR, F., ELASSALI, R., et al. Performance of universal filtered multicarrier channel estimation with different pilots arrangements. In *IEEE 5G World Forum (5GWF)*. Santa Clara (CA, USA), 2018, p. 327–332. DOI: 10.1109/5gwf.2018.8517030

[26] BAMBHANIYA, A. B., RATHOD, J. M. Research on various pilot pattern design for channel estimation in OFDM system. *International Journal of Applied Engineering Research*, 2017, vol. 12, no. 24, p. 14403–14407. DOI: 10.1049/el:20000714

About the Authors . . .

He HE received the B.E. in Electrical and Electronics Engineering from Dalian Maritime University, Dalian, China, in 2018 and the M.E. degree in Electrical and Electronics Engineering from Chiba University, Chiba, Japan in 2020. He is now doing his Ph.D. program in the Chiba University. His research interests include machine learning and development of next generation communication algorithm.

Shun KOJIMA received the B.E. and M.E. degrees in Electrical and Electronics Engineering from Chiba University, Japan, in 2017 and 2018, respectively, where he is currently pursuing the Ph.D. degree with the Graduate School of Engineering. His research interests include MIMO, cooperative communications, adaptive modulation and coding, neural networks, and channel estimation. He received the Best Paper Award from the 26th International Conference on Software, Telecommunications and Computer Networks (SoftCOM2018).

Takaki OMURA received the B.E. and M.E. degrees in Electrical and Electronics Engineering from Chiba University, Japan, in 2018 and 2020, respectively.

Kazuki MARUTA received the B.E., M.E., and Ph.D. degrees in Engineering from Kyushu University, Japan, in 2006, 2008 and 2016, respectively. From 2008 to 2017, he was with NTT Access Network Service Systems Laboratories and was engaged in the research and development of interference compensation techniques for future wireless communication systems. From 2017 to 2020, he was an Assistant Professor in the Graduate School of Engineering, Chiba University. He is currently a Specially Appointed Associate Professor in the Academy for Super Smart Society, Tokyo Institute of Technology. His research interests include MIMO, adaptive array signal processing, channel estimation, medium access control protocols and moving networks. He is a member of the IEEE and The Institute of Electronics, Information and Communication Engineers (IEICE). He received the IEICE Young Researcher's Award in 2012, the IEICE Radio Communication Systems (RCS) Active Researcher Award in 2014, APMC2014 Prize, the IEICE RCS Outstanding Researcher Award in 2018, and the IEEE ICCE Excellent Paper Award in 2021. He was a co-recipient of the IEICE Best Paper Award in 2018, SoftCOM2018 Best Paper Award and APCC2019 Best Paper Award.

Chang-Jun AHN received the Ph.D. degree from the Department of Information and Computer Science from Keio University, Japan, in 2003. From 2001 to 2003, he was a Research Associate with the Department of Information and Computer Science, Keio University. From 2003 to 2006, he was with the Communication Research Laboratory, Independent Administrative Institution (National Institute of Information and Communications Technology). In 2006, he was on assignment with ATR Wave Engineering Laboratories. In 2007, he was a Lecturer with the Faculty of Information Sciences, Hiroshima City University. He is currently a Professor with the Graduate School of Engineering, Chiba University. His research interests include OFDM, MIMO, digital communication, channel coding, signal processing for telecommunications, and wireless power transfer. He served as an associate editor of the IEICE Trans. on Fundamentals. From 2005 to 2006, he was an expert committee member for emergence communication committee, Shikoku Bureau of Telecommunications, Ministry of Internal Affairs and Communications (MIC), Japan. Dr. Ahn received the ICF research grant award for Young Engineer in 2002, the Funai Information Science Award for Young Scientist in 2003, the Distinguished Service Award from Hiroshima City in 2010, IEEE SoftCOM2018 Best Paper Award in 2018, IEEE APCC2019 Best Paper Award in 2019, IEICE ICETC2020 Best Paper Award in 2020, and Journal of Signal Processing Best Paper Award in 2021. He is a senior member of IEICE and IEEE.